Chemical Science

EDGE ARTICLE

View Article Online
View Journal | View Issue

Cite this: *Chem. Sci.*, 2015, **6**, 1018

Chelation-induced diradical formation as an approach to modulation of the amyloid-β aggregation pathway†

Meghan R. Porter,[a] Akiko Kochi,[bc] Jonathan A. Karty,[a] Mi Hee Lim*[cd] and Jeffrey M. Zaleski*[a]

Current approaches toward modulation of metal-induced Aβ aggregation pathways involve the development of small molecules that bind metal ions, such as Cu(II) and Zn(II), and interact with Aβ. For this effort, we present the enediyne-containing ligand (*Z*)-*N*,*N*′-bis[1-pyridin-2-yl-meth(*E*)-ylidene]oct-4-ene-2,6-diyne-1,8-diamine (**PyED**), which upon chelation of Cu(II) and Zn(II) undergoes Bergman-cyclization to yield diradical formation. The ability of this chelation-triggered diradical to modulate Aβ aggregation is evaluated relative to the non-radical generating control pyridine-2-ylmethyl-(2-{[(pyridine-2-ylmethylene)-amino]-methyl}-benzyl)-amine (**PyBD**). Variable-pH, ligand UV-vis titrations reveal $pK_a = 3.81(2)$ for **PyBD**, indicating it exists mainly in the neutral form at experimental pH. Lipinski's rule parameters and evaluation of blood–brain barrier (BBB) penetration potential by the PAMPA–BBB assay suggest that **PyED** may be CNS+ and penetrate the BBB. Both **PyED** and **PyBD** bind Zn(II) and Cu(II) as illustrated by bathochromic shifts of their UV-vis features. Speciation diagrams indicate that Cu(II)–**PyBD** is the major species at pH 6.6 with a nanomolar K_d, suggesting the ligand may be capable of interacting with Cu(II)–Aβ species. In the presence of $Aβ_{40/42}$ under hyperthermic conditions (43 °C), the radical-generating **PyED** demonstrates markedly enhanced activity (2–24 h) toward the modulation of Aβ species as determined by gel electrophoresis. Correspondingly, transmission electron microscopy images of these samples show distinct morphological changes to the fibril structure that are most prominent for Cu(II)–Aβ cases. The loss of CO_2 from the metal binding region of Aβ in MALDI-TOF mass spectra further suggests that metal–ligand–Aβ interaction with subsequent radical formation may play a role in the aggregation pathway modulation.

Received 2nd July 2014
Accepted 30th October 2014

DOI: 10.1039/c4sc01979b

www.rsc.org/chemicalscience

Introduction

Alzheimer's disease (AD) is the most common form of dementia, affecting over 24 million people worldwide.[1] It is estimated that this number will nearly double by 2030, partly due to demographic aging resulting from improved healthcare.[1] The disease presence and progression are pathologically characterized by accumulation of misfolded amyloid-β (Aβ) peptides deriving from β- and γ-secretase cleavage of the amyloid precursor protein (APP)[2–4] to produce $Aβ_{40}$ and $Aβ_{42}$ that self-assemble through hydrophobic interactions to form oligomers, protofibrils, fibrils, and ultimately, insoluble plaques.[4–6] It has been proposed that Aβ plaque accumulation may arise from an imbalance in Aβ production and clearance (*i.e.*, amyloid cascade hypothesis);[4,7–9] accumulation of these peptides alone can impair neuronal mitochondrial function, leading to oxidative stress, inflammation, and the neurodegeneration commonly associated with AD (*i.e.*, oxidative stress hypothesis).[4,10–12] In addition to self-aggregation, miscompartmentalization and dyshomeostasis of metals are found in AD-afflicted brains. In particular, elevated levels of metals, such as Cu, Zn, and Fe, are observed in Aβ plaques.[3–5,13–19] Metal binding to Aβ is shown to facilitate peptide aggregation and in the case of redox active metal ions, reactive oxygen species (ROS) can be generated *via* Fenton-like reactions, leading to oxidative stress.[4,5,17,19–24]

On the basis of the observed metal ion dyshomeostasis, metal–Aβ interaction, and metal-involved Aβ reactivity, there has been considerable interest in the development of metal chelators capable of regulating metal ion distribution distribution and amyloid pathology. For example, the hydroxyquinoline-based antifungal drug clioquinol (CQ) decreased Aβ deposits and showed improved cognition in Phase II clinical

[a]*Department of Chemistry, Indiana University, Bloomington, Indiana 47405, USA. E-mail: zaleski@indiana.edu*

[b]*Department of Chemistry, University of Michigan, Ann Arbor, Michigan 48109, USA*

[c]*Department of Chemistry, Ulsan National Institute of Science and Technology (UNIST), Ulsan 689-798, Korea. E-mail: mhlim@unist.ac.kr*

[d]*Life Sciences Institute, University of Michigan, Ann Arbor, Michigan 48109, USA*

† Electronic supplementary information (ESI) available: Details of experimental procedures and supplementary figures and tables. See DOI: 10.1039/c4sc01979b

trials for AD, in part due to its ability to inhibit binding of Zn(II) and Cu(II) to Aβ *via* chelation.[25–27] Moreover, the second generation 8-hydroxyquinoline ionophore PBT2 also improved learning and memory by redistributing Cu(II) and Zn(II) and lowered cerebrospinal fluid levels of Aβ in Phase II clinical trials.[28,29]

Although CQ and PBT2 have presented noticeable effects on metal redistribution and Aβ clearance, the relationship between metal-associated Aβ (metal–Aβ) species and AD pathogenesis is still unclear, thus new efforts on developing chemical tools for specifically studying metal–Aβ species have been made.[21,24,30–33] For example, the rational design of chelators containing dimethylaniline and polydentate motifs using nitrogen and oxygen donor atoms for metal ions has led to blood–brain barrier (BBB) permeable compounds that modulate metal-induced Aβ aggregation, reduce Cu–Aβ ROS formation, demonstrate antioxidant activity, and/or decrease metal–Aβ toxicity *in vitro*.[30,32–34]

Our latest approach to bifunctional chelators for Aβ modification derives from drugs such Fe-Bleomycin or hydroxyl radical footprinting reagents that act *via* Fenton chemistry and perform H-atom abstraction from the ribose ring of DNA leading to strand scission.[35,36] Similarly, enediyne natural products such as calicheamicin that generate a potent 1,4-phenyl diradical also affect strand scission by H-atom abstraction. Radical reactions of these types however, are not limited to DNA substrates. Rather, radical-mediated footprinting is an established methodology for evaluating protein structure *via* solvent accessible reactivity,[37] as well as for mapping protein–protein and protein–DNA interactions.[38–47] Generation of ROS by reaction with redox active Fe, Cu, and Mn-complexes[38,48–58] in the presence of reductant leads to controlled backbone or side chain attack which can be used to evaluate regions of macromolecular interface. While ribose ring radical strand breaks in DNA are generally due to H-atom abstraction from relatively weak tertiary C–H bonds[38] that are statistically plentiful and readily accessible,[59] H-atom abstraction from proteins is more complex. Direct H-abstraction from the α-carbon and side chain-assisted H-abstraction both lead to backbone cleavage,[59–61] but poor solvent permeability and the statistical probability of extensive side chain oxidation make this process less prevalent.[37,39,46,47,59,62] Somewhere between these limits lies calicheamicin which performs α-H abstraction from the protector protein CalC at Gly-113, cleaving the protein in a radical self-resistance mechanism.[63]

With this backdrop, we envisioned a bifunctional agent that could attack Aβ aggregates by initially chelating Aβ-bound metal ions to disrupt the peptide structure and subsequently using this chelation event to induce diradical formation that would further modify the remaining Aβ aggregates. We have shown that the compound (*Z*)-*N*,*N*′-bis[1-pyridin-2-yl-meth(*E*)-ylidene] oct-4-ene-2,6-diyne-1,8-diamine (**PyED**) (Fig. 1) binds a wide array of metal ions such as Mg,[64] Cu, Fe, and Zn and these complexes may be thermally activated to yield a potent 1,4-diradical intermediate. Our experience with enediyne activation *via* metal coordination[64–66] and photochemical[67–69] diradical formation has taught us that these molecular frameworks are capable of both H-atom abstraction[64,66,67] and addition/polymerization reactions[68,69] depending upon the substrate and radical–radical coupling proximity. Additionally, **PyED** has demonstrated enhanced activity under clinically relevant hyperthermic conditions (42.5 °C).[70] Although hyperthermic treatments have not commonly been applied in the field of AD, hyperthermia has been established as a method to enhance therapeutic efficiency when used in combination with other cancer treatments both *in vitro*[71–75] and *in vivo*[75–78] (≤45.5 °C). Thus, herein we report the application of such reactions to metal-bound (Cu(II), Zn(II)) Aβ aggregates by administration of **PyED** at physiological (37 °C) and hyperthermic (43 °C) temperatures relative to the non-radical generating control pyridine-2-ylmethyl-(2-{[(pyridine-2-ylmethylene)-amino]-methyl}-benzyl)-amine, **PyBD** (Fig. 1).

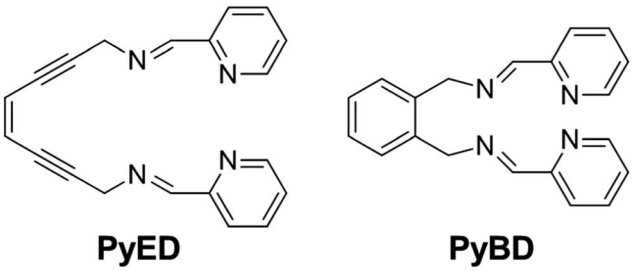

Fig. 1 Structures of radical-generating enediyne and cyclized control ligands employed for modulation of Aβ species.

Results and discussion

Rationale and characterization of PyED and PyBD used for modulating metal–Aβ species

The reactive compounds **PyED** (chelation + radical generation) and **PyBD** (chelation alone) for the modulation of Aβ species were synthesized and characterized by their ^{1}H, ^{13}C NMR, and mass signatures according to literature precedent.[64] Cyclization of **PyED** by Cu(II) or Zn(II) chelation was investigated in MeOH and occurs within 4 h at 37 °C upon radical trapping with 1,4-cyclohexadiene and extraction with $NaBH_4$ (12 equiv.)/EDTA (pH 10.6).[64] The ^{13}C NMR feature at δ 128 ppm and ESI-MS (*m*/*z*: 319.2) are diagnostic of cyclized product formation indicating **PyED** undergoes rapid radical formation in the presence of Cu(II) or Zn(II). Variable-pH UV-visible (UV-vis) titrations were conducted to evaluate the protonation state of the ligand in solution, particularly at physiologically relevant pH (pH = 7.4).[34,79,80] In light of the fact that **PyED** slowly generates reactive radicals at ambient temperature over the timescale of the measurement (4–5 h), speciation was determined using the nonreactive, cyclized control **PyBD**. Titration results indicate a single acid ionization constant (pK_a) for **PyBD** ($pK_a = 3.81(2)$), suggesting that neutral and monoprotonated forms of the ligand may be present in solution depending on pH. Furthermore, the solution speciation diagram reveals that **PyBD** is expected to exist mainly in the neutral form at pH 7.4 (Fig. 2).

In an effort to establish the drug-likeness of **PyED** and its potential to penetrate the BBB, Lipinski's rule parameters (MW < 450, *c* log *P* < 5.0, HBA < 10, HBD < 5) and the log BB were

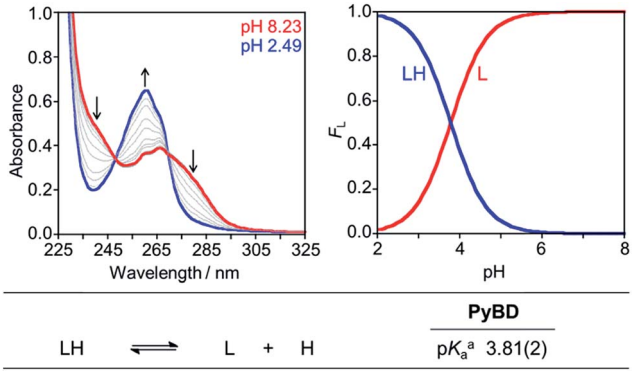

Fig. 2 Solution speciation of **PyBD** (50 μM). Left: UV-vis spectra in the range of pH 2–8. Right: solution speciation diagram (F_L = fraction of compound in given protonation state). Bottom: acidity constants of L (L = **PyBD**) with charges omitted for clarity. Speciation was performed at room temperature with I = 0.1 M NaCl. [a]Error in the last digit is indicated in parentheses.

Table 1 Values for Lipinski's rules and others for **PyED**

Calculation[a]	**PyED**	Lipinski rule parameters and others
MW	312.37	450
c log *P*	1.01	5.0
HBA	4	10
HBD	0	5
PSA	50.5	90 Å^2
log BB	−0.464	0.3 (readily crosses the BBB) −1.0 (poorly distributed in the brain)
−log P_e[b]	4.9 ± 0.1	
CNS± prediction[c]	CNS+	−log P_e 5.4 (CNS+) −log P_e 5.7 (CNS−)

[a] MW, molecular weight; *c* log *P*, calculated logarithm of the octanol–water partition coefficient; HBA, hydrogen-bond acceptor atoms; HBD, hydrogen-bond donor atoms; PSA, polar surface area; log BB = −0.0148 × PSA + 0.152 × *c* log *P* 0.130. [b] The values of −log P_e were measured by the parallel artificial membrane permeability assay (PAMPA). [c] CNS+ compounds have the ability to permeate the BBB and target the CNS, while CNS− compounds have poor permeability through the BBB and therefore, their bioavailability into the CNS is considered minimal.

evaluated (Table 1).[81–84] The resulting values (MW = 312.37, *c* log *P* = 1.01, HBA = 4, HBD = 0) indicate **PyED** has drug-like characteristics as well as possible BBB permeability (Table 1). In order to verify the predicted ability of **PyED** to penetrate the BBB, an *in vitro* PAMPA–BBB assay was performed following literature procedure.[34,81,85] Using the empirical classification for BBB-permeable molecules, the measured permeability value, −log P_e, for **PyED** (−log P_e = 4.9 ± 0.1) suggests **PyED** may be likely to penetrate the BBB.

Metal binding properties of PyED and PyBD

Divalent metal binding of **PyED** and **PyBD** at 0 °C was demonstrated by bathochromic shifts of their UV-vis features (**PyED** λ = 264 nm; **PyBD** λ = 272 nm) upon addition of $ZnCl_2$ or $CuCl_2$ (1 equiv.) in ethanol (Fig. S1†). At 1 equiv. of MCl_2, the absorption spectra of **PyBD** show the formation of distinct metallated species with larger bathochromic shifts observed for Cu(II) binding relative to Zn(II). For the more flexible chelate **PyED**, these shifts are somewhat less pronounced and indicate parallel, but slightly weaker ligand binding under these unactivating conditions (0 °C). The apparent trend of enhanced Cu(II) binding relative to Zn(II) is consistent with those observed for N-donor functionalities within a range of flexible ligands.[25,86–88]

Although the neutral form of **PyBD** is the major species in solution at physiological pH (*vide supra*), variable-pH UV-vis titrations were also conducted to elucidate complexation and binding properties of **PyBD** with Cu(II) in solution at ambient temperature and the proposed local pH for Cu(II)–Aβ species (pH = 6.6) (Fig. 3, left). Based on the pK_a value determined for **PyBD** and these titration results, the stability constants (log β) for the these complexes were determined to be 12.2(8) and 4.4(8) for CuL and Cu(LH), respectively. A solution speciation diagram was modeled using these stability constants and suggests complexation of **PyBD** with Cu(II) occurs in a 1 : 1 metal : ligand ratio. While neutral and protonated forms of Cu(II)–**PyBD** may exist at different pH values, the data indicate that the neutral Cu(II)–**PyBD** form is the major species at pH 6.6 (Fig. 3, right). Additionally, the concentration of free Cu(II) in solution at pH 6.6 yields a *p*Cu value of 8.3(4) (*p*Cu = −log $[Cu(II)]_{unbound}$). The *p*Cu magnitude suggests an approximate K_d for Cu(II)–**PyBD** to be *ca.* nanomolar. When considered with the reported K_d values for Cu(II)–Aβ species (picomolar to nanomolar range),[4,5,17,19–21,24,89] this approximate dissociation constant indicates that **PyBD** may be able to compete for Cu(II) binding in Cu(II)–Aβ species.

To estimate the ability of **PyED** to bind Cu(II) in the presence of other biologically relevant metal ions such as Ca(II), Co(II), Fe(II), Fe(III), Mg(II), Mn(II), Ni(II), and Zn(II), selectivity was evaluated for the unreactive model compound **PyBD** by a

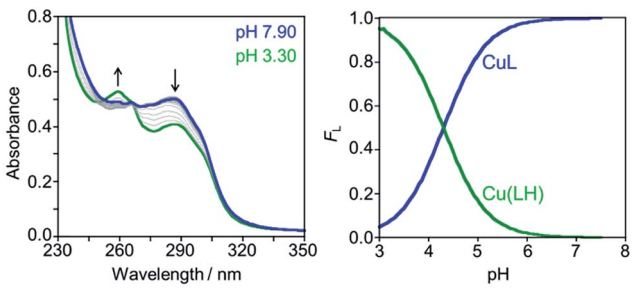

Fig. 3 Solution speciation of the Cu(II)–**PyBD** complex. Left: UV-vis spectra in the range of pH 3–8 ([Cu(II)]/[**PyBD**] = 1 : 1; $[Cu(II)]_{total}$ = 50 μM). Right: solution speciation diagram (F_{Cu} = fraction of free Cu and Cu complexes). Bottom: stability constants of the Cu(II)–**PyBD** complex with charges admitted for clarity. Titrations were performed at room temperature with I = 0.1 M NaCl. [a]Error in the last digit is indicated in parentheses.

competitive UV-vis absorption assay (Fig. S2†). Even in the presence of a large excess of competing metal ion, **PyBD** displays good selectivity for Cu(II) over Ca(II), Co(II), Mg(II), Mn(II), and Ni(II), while significant binding is shown in the presence of Fe(II) and Fe(III) (Fig. S2†). The observation that **PyBD** demonstrates selectivity for Cu(II) over Zn(II) leads to the expectation that modulation of Cu(II)-bound Aβ species *via* metal chelation and subsequent radical generation by **PyED** may be more prominent than for the Zn(II)-bound species (*vida infra*). Overall, the tetradentate pyridine–imine binding moiety of **PyBD** and **PyED** may be desirable for reacting with Cu(II)–Aβ species over other biologically relevant divalent metal ions.

Effect of PyED and PyBD on metal-free and metal-triggered Aβ aggregation *in vitro*

In order to assess the ability of bifunctional **PyED** to modulate metal-induced $A\beta_{40}$ and $A\beta_{42}$ aggregation pathways, *in vitro* disaggregation and inhibition experiments were conducted (Scheme 1).[32,79,80] For comparison to **PyED** reactivity, the influence of monofunctional **PyBD** on Aβ aggregation was also examined. Disaggregation assays were designed to investigate the potential of both **PyED** and **PyBD** to structurally alter preformed metal-free and metal-associated Aβ aggregates (Fig. 4 and 5), while inhibition experiments probed the compounds' ability to control the formation of metal-free and metal-induced Aβ aggregates (Fig. S3 and S4†). The resultant Aβ species were characterized using gel electrophoresis followed by Western blot with an anti-Aβ antibody (6E10), and morphological changes were monitored by transmission electron microscopy (TEM).[32,80]

For preformed metal-free and metal-associated $A\beta_{40}$ and $A\beta_{42}$ aggregates, **PyED** and **PyBD** exhibit differing disaggregation capabilities (Fig. 4 and 5). In the case of Zn(II)– and Cu(II)–$A\beta_{40}$ samples treated with **PyED**, Aβ species with an increasing range of molecular weights (MW) are observed at both 37 and 43 °C between 2 and 8 h, while a decrease in signal intensity occurs between 8 and 24 h for samples incubated at 37 °C (Fig. 4A, lanes 5 and 8). Interestingly, variable reactivity of **PyED** with preformed Zn(II)–$A\beta_{40}$ aggregates was detected at 43 °C. Addition of **PyED** presented an increasing distribution of MW throughout the time course (Fig. 4A, lane 5). In contrast, treatment of metal–$A\beta_{40}$ samples with **PyBD** leads to the generation of lower MW species (MW ≤ 25 kDa) over the 24 h period (Fig. 4A, lanes 6 and 9). These data suggest that **PyBD** only slightly affects the transformation of preformed metal–Aβ aggregates, indicating that the introduction of radical formation upon metal binding by **PyED** may be a key factor in the generation of metal-associated Aβ species exhibiting a different array of MW. Additionally, the reduction of gel band intensities in Cu(II)–$A\beta_{40}$ samples incubated with **PyED** for 24 h may imply the occurrence of further aggregation over time. These results are markedly different than those observed for metal-free samples incubated with **PyED** or **PyBD** which demonstrate overall minimal disaggregation activity, with the exception of 8 h incubation under hyperthermic conditions. This modest metal-free activity is expected due to the absence of both chelation and chelation-induced radical generation pathways (Fig. 4A, lane 2). In the absence of divalent metals, initiation of thermally-induced **PyED** cyclization is slow,[64] leading to limited radical formation under these conditions.

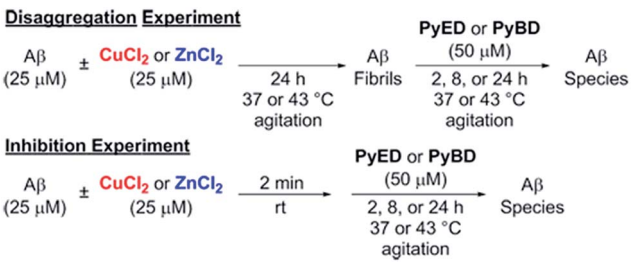

Scheme 1 Experimental set-up for $A\beta_{40}$ and $A\beta_{42}$ disaggregation and inhibition assays.

The trends in the gel analysis are consistent with TEM images of preformed metal–$A\beta_{40}$ aggregates treated with **PyED**. At 37 °C, TEM images of metal–$A\beta_{40}$ show a mixture of fibrillar and amorphous structure types, while at 43 °C amorphous Aβ morphologies are dominant. In comparison, parallel samples incubated with **PyBD** exhibit fibrillar structures similar to those under compound-free conditions at both temperatures (Fig. 4B and C). Since **PyED** and **PyBD** show minimal change in the morphology of metal-free $A\beta_{40}$ aggregates relative to untreated samples, this suggests that variations in the fibrillar morphology may derive from chelation and chelation-induced radical mechanisms (Fig. 4B and C).

The ability of **PyED** and **PyBD** to transform preformed $A\beta_{42}$ aggregates was also examined (Fig. 5). Relative to analogous $A\beta_{40}$ samples, a similar trend in both **PyED** and **PyBD** reactivity with $A\beta_{42}$ was confirmed by gel electrophoresis. $A\beta_{42}$ species with a wide distribution of MW are observed with **PyED**-treated, metal-associated $A\beta_{42}$ aggregates over the course of 24 h at both temperatures (Fig. 5A, lanes 5 and 8), while low reactivity is visualized in metal–$A\beta_{42}$ samples incubated with **PyBD** (lanes 6 and 9). In the case of metal-free conditions, a slightly different ensemble of $A\beta_{42}$ MW are produced relative to the untreated control upon addition of **PyED** or **PyBD** (lanes 1–3). In addition to these trends, the TEM images reveal that analogous to $A\beta_{40}$, addition of **PyED** to metal–$A\beta_{42}$ samples induces changes in the morphology of preformed aggregates. Metal-treated $A\beta_{42}$ exposed to either **PyED** or **PyBD** show thinner fibrils of various lengths (37 and 43 °C), as well as more amorphous species (37 °C) than observed in compound-free samples (Fig. 5B and C). As demonstrated for $A\beta_{40}$, no distinct morphology changes are observed in the metal-free $A\beta_{42}$ samples treated with either ligand when compared to the untreated sample, indicating the importance of metal chelation in the disaggregation pathway.

In an effort to evaluate whether chelation and radical generation can influence fibril assembly, the effect of **PyED** and **PyBD** on modulation of the Aβ aggregation pathway was investigated (Fig. S3 and S4†). Upon incubation of Zn(II) and $A\beta_{40}$ with **PyED**, an increasing dispersion of various MW was visualized by gel analysis over prolonged exposures of up to 24 h (Fig. S3,† lane 5). In comparison, samples containing Cu(II),

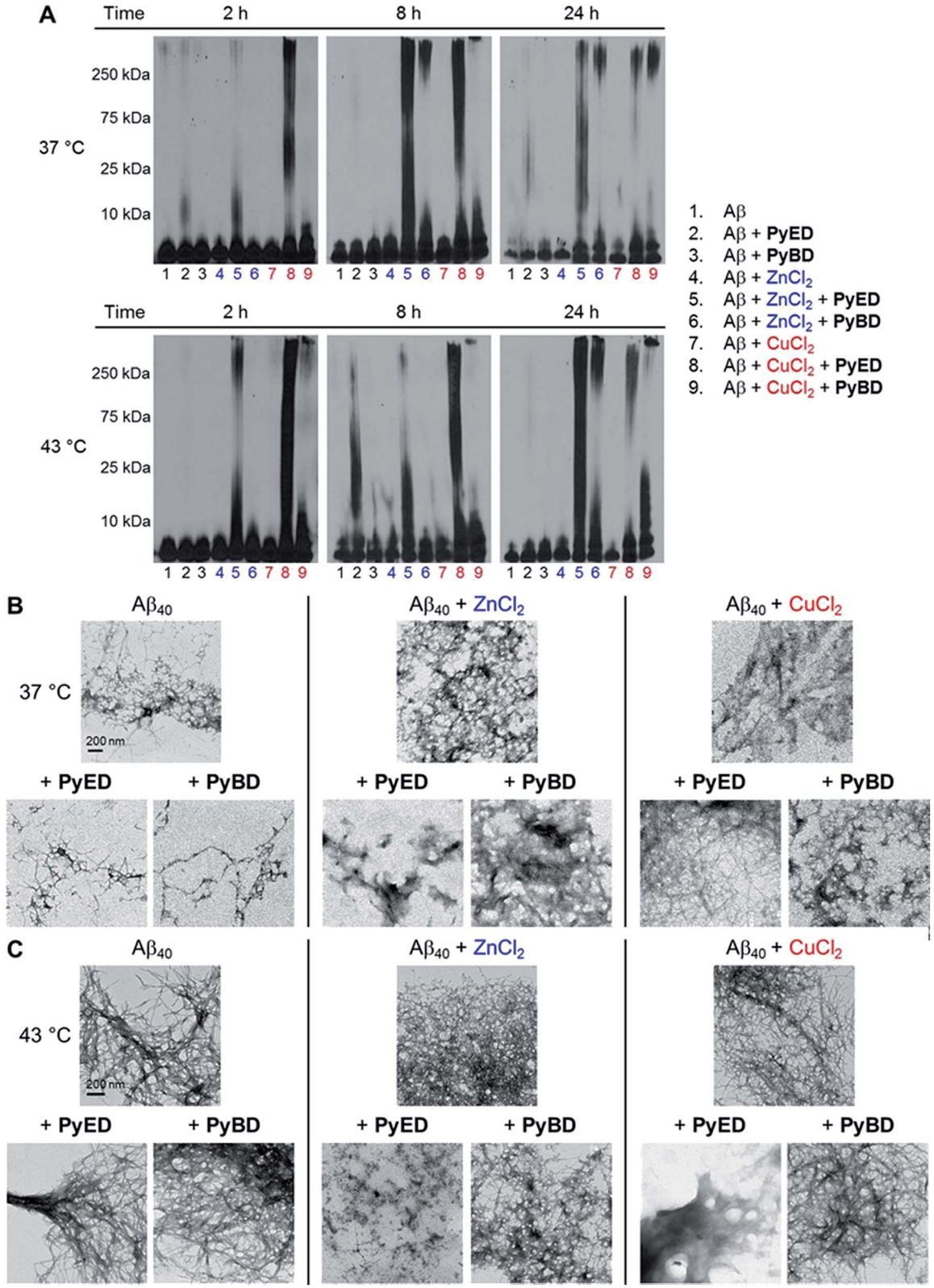

Fig. 4 Reactivity of **PyED** and **PyBD** with preformed $A\beta_{40}$ aggregates. (A) Analysis of resultant $A\beta_{40}$ species by gel electrophoresis with Western blot using an anti-Aβ antibody (6E10). TEM images of the samples incubated for 24 h at (B) 37 °C or (C) 43 °C. Experimental conditions: [Aβ] = 25 μM; [$CuCl_2$ or $ZnCl_2$] = 25 μM; [**PyED** or **PyBD**] = 50 μM; 2, 8, 24 h incubation at 37 or 43 °C; pH 7.4 (metal-free and Zn(II)) or pH 6.6 (Cu(II)); constant agitation.

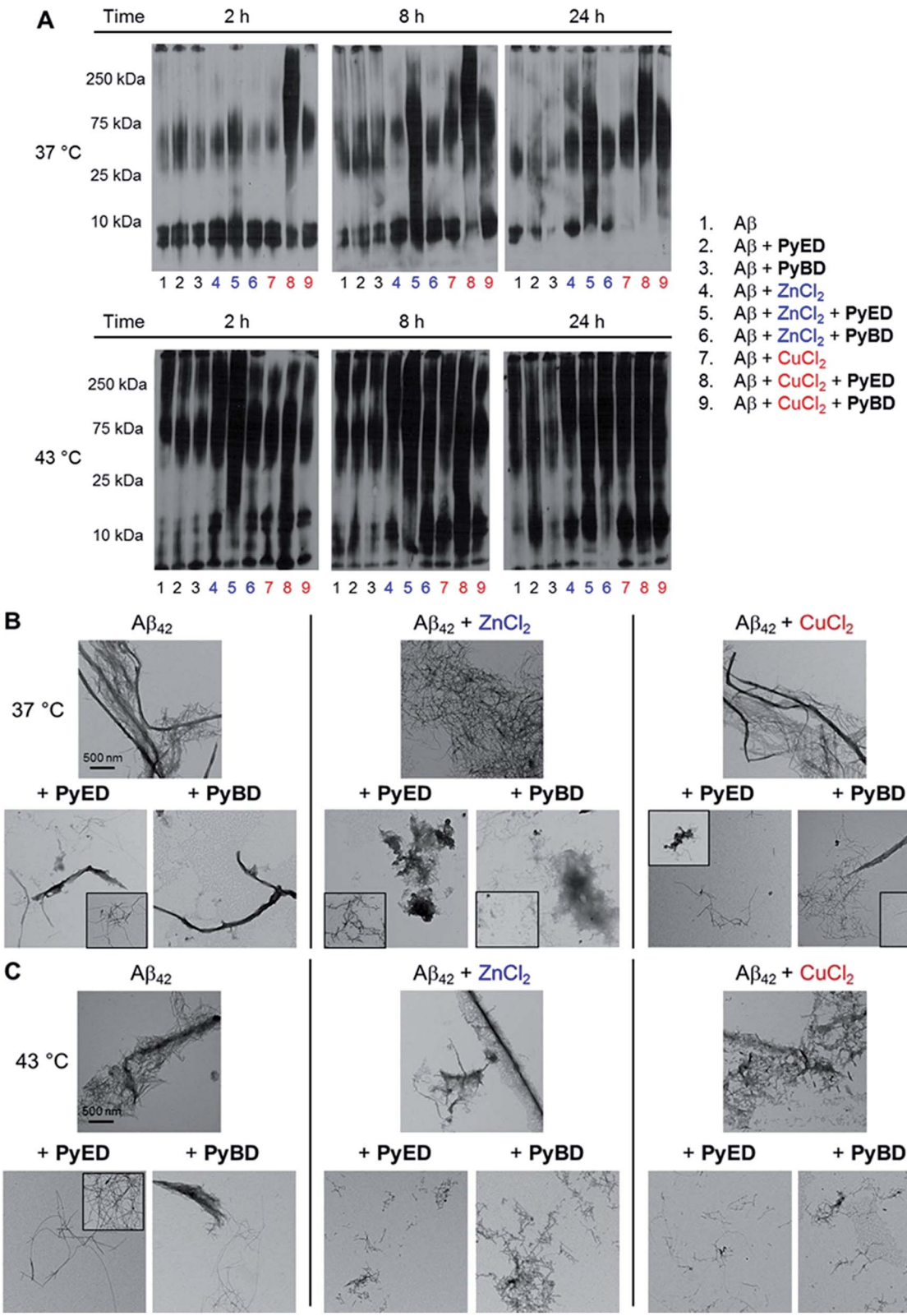

Fig. 5 (A) Analysis of resultant $A\beta_{42}$ species by gel electrophoresis with Western blot using an anti-Aβ antibody (6E10). TEM images of samples incubated for 24 h at (B) 37 °C or (C) 43 °C. Experimental conditions: [Aβ] = 25 μM; [$CuCl_2$ or $ZnCl_2$] = 25 μM; [**PyED** or **PyBD**] = 50 μM; 2, 8, 24 h incubation at 37 or 43 °C; pH 7.4 (metal-free and Zn(II)) or pH 6.6 (Cu(II)); constant agitation.

$A\beta_{40}$, and **PyED** generate different smearing patterns than those of the analogous Zn(II)–$A\beta_{40}$ samples (lanes 5 and 8). Similar to the disaggregation results, the gel band intensities of the Cu(II)–$A\beta_{40}$ samples also decrease between 8 and 24 h incubation time at both 37 and 43 °C, suggesting the possibility of further aggregation over long incubation times. The **PyED** inhibition activity compares favorably with that of **PyBD**, where only a slight modulation of the metal-induced aggregation pathway is observed (lanes 6 and 9), while exposure of metal-free $A\beta_{40}$ to either **PyED** or **PyBD** results in little to no activity (lanes 2 and 3). Thus, analogous to the disaggregation results, these data indicate that bifunctional **PyED** exhibits greater inhibition of metal-induced Aβ aggregation compared to monofunctional **PyBD**. These findings are supported by TEM images of $A\beta_{40}$ samples incubated at 43 °C that reveal smaller, amorphous Aβ species in the presence of divalent metal ions and **PyED** (Fig. S3C†). Importantly, no significant morphological changes are observed in the metal-free Aβ samples exposed to either **PyED** or **PyBD**. As expected, the trend in the inhibition of $A\beta_{42}$ aggregation upon addition of **PyED** or **PyBD** is comparable to that of $A\beta_{40}$ (Fig. S4†). Significant modification of the aggregation pathway is only visualized for metal-associated Aβ species treated with **PyED** (Fig. S4A,† lanes 5 and 8). Additionally, TEM images reveal that thinner fibrils and/or amorphous aggregates are generated in **PyED**-treated metal–$A\beta_{42}$ samples compared to compound-free conditions (Fig. S4B and C†). Taken together, the disaggregation and inhibition results reveal the enhanced ability of **PyED** (*vs.* **PyBD**) to variably modulate metal-free and metal-induced Aβ aggregation.

From the data available on a range of molecular structures, modulation of Aβ species may derive from the differential interaction between the ligand frameworks and monomeric Aβ peptide.[4,30,32] To evaluate the degree of this interaction, Aβ was incubated with **PyED** or control ligand **PyBD** at 0 °C for 2 h in a ratio of 6 : 1 ligand : Aβ peptide ([Aβ] = 100 μM).[30] The resulting species were analyzed using native nanoelectrospray ionization-mass spectrometry by comparison to the established Aβ-interacting neuropeptide Leucine-enkephalin (Leu-enk).[90] No ligand–Aβ species were detected and no significant differences were observed between the spectra obtained upon incubation with **PyED** or **PyBD**, suggesting neither ligand framework appreciably binds Aβ relative to Leu-enk.

Overall, the data suggest that the disparate capability of **PyED** to regulate Aβ aggregation is due to a combination of metal extraction from Aβ, interaction of ligand with metal-bound Aβ species, and induction of radical-mediated modification of the peptide aggregation pathway. In support of the interaction of **PyED** and **PyED** with metal-bound Aβ species at 43 °C, photo-induced loss of HCO_2 from M(II)–Aβ disaggregation samples and subsequent loss of CO_2 (Cu(II)–Aβ only) on the b-ions is observed by MALDI-TOF-TOF, whereas the corresponding y-ions appear to be intact (Fig. S5 and Tables S1–S3†). Moreover, the b_7 ion reveals that CO_2 loss occurs N-terminal to aspartate, D7. In addition, MALDI-TOF data show that HCO_2 loss is only operative upon incubation (4–8 h) of the components Aβ, metal ion (Cu(II) or Zn(II)), and ligand (**PyBD** or **PyED**) (Fig. S6–S8†). This loss of HCO_2 from M(II)–Aβ and subsequent loss of CO_2 (Cu(II)–Aβ only) is also observed in the analogous 37 °C disaggregation samples (Fig. S9–S11†). Importantly, rapid addition of any of the pair of components with the same incubation time, or the mixture of three components with no incubation does not result in any detectable photo-induced loss of CO_2. This indicates that metal and ligand must be co-localized within the metal binding consensus sequence (1–16) and is consistent with CO_2 loss mechanisms from photo-induced redox and ESI electron capture/detachment of Cu and Zn bound peptides.[91–94]

While evidence for the interaction among Aβ, metal ions, and **PyED** or **PyBD** is suggested for the Aβ modulation pathway, and radical-induced peptide fragmentation as part of the overarching Aβ degradation process is also proposed, detection of specific, low MW fragments is more elusive. Peptidic cleavage by α-H-atom abstraction and subsequent detection of fragments by mass spectrometry is complicated by solvent accessibility and side-chain reactivity which diversify product distribution and reduce the abundances of individual species. The absence of individual peptide fragments, however, does not preclude radical damage to Aβ as all of these radical reaction pathways will lead to structural changes in metal-bound Aβ aggregates. Thus, the enhanced reactivity of **PyED** compared to **PyBD** towards metal–Aβ species is reflective of the broader role radicals may play in the modulation of overall Aβ structure.

Conclusions

Approaches to modulate the aggregation pathway are at the forefront of current small molecule designs for AD therapy. The ensemble of existing methodologies encompasses metal chelation and interruption of peptide aggregation by ligand interaction with Aβ, as well as targeting metal–Aβ ternary complex formation as disruption mechanisms. Here we demonstrate a bifunctional approach that combines metal chelation and active radical generation to affect Aβ aggregation. Our results indicate that the ligand–metal–Aβ interaction with subsequent radical generation is a relatively rapid (2 h at 43 °C) mechanism for influencing Aβ structural integrity and thus, the aggregation pathway. This outcome may lead to new hybrid molecular constructs designed to take advantage of several Aβ interaction modes in order to achieve rapid Aβ species modulation.

Acknowledgements

This work is supported by the National Science Foundation (CHE-1265703) (to J.M.Z.); the Ruth K. Broad Biomedical Foundation, the DGIST R&D Program of the Ministry of Science, ICT and Future Planning of Korea (14-BD-0403), and the National Research Foundation of Korea grant funded by the Korean government (MSIP) (NRF-2014R1A2A2A01004877) (to M.H.L.). The authors thank Joan M. Walker for acquiring the $A\beta_{40}$ TEM images.

Notes and references

1 Alzheimer's Association, *Alzheimers Dement.*, 2012, **8**, 131–168.
2 F. M. LaFerla, K. N. Green and S. Oddo, *Nat. Rev. Neurosci.*, 2007, **8**, 499–509.
3 R. Jakob-Roetne and H. Jacobsen, *Angew. Chem., Int. Ed.*, 2009, **48**, 3030–3059.
4 K. P. Kepp, *Chem. Rev.*, 2012, **112**, 5193–5239.
5 M. G. Savelieff, A. S. DeToma, J. S. Derrick and M. H. Lim, *Acc. Chem. Res.*, 2014, **47**, 2475–2482.
6 Y. Miller, B. Ma and R. Nussinov, *Chem. Rev.*, 2010, **110**, 4820–4838.
7 K. Blennow, M. J. de Leon and H. Zetterberg, *Lancet*, 2006, **368**, 387–403.
8 M. P. Mattson, *Nature*, 2004, **430**, 631–639.
9 E. Karran, M. Mercken and B. De Strooper, *Nat. Rev. Drug Discovery*, 2011, **10**, 698–712.
10 M. F. Galindo, I. Ikuta, X. Zhu, G. Casadesus and J. Jordan, *J. Neurochem.*, 2010, **114**, 933–945.
11 J. P. Blass, *Ann. N. Y. Acad. Sci.*, 2000, **924**, 170–183.
12 M. Dumont and M. F. Beal, *Free Radical Biol. Med.*, 2011, **51**, 1014–1026.
13 K. J. Barnham and A. I. Bush, *Curr. Opin. Chem. Biol.*, 2008, **12**, 222–228.
14 A. I. Bush, W. H. Pettingell, G. Multhaup, M. d. Paradis, J.-P. Vonsattel, J. F. Gusella, K. Beyreuther, C. L. Masters and R. E. Tanzi, *Science*, 1994, **265**, 1464–1467.
15 A. I. Bush, *Trends Neurosci.*, 2003, **26**, 207–214.
16 B. R. Roberts, T. M. Ryan, A. I. Bush, C. L. Masters and J. A. Duce, *J. Neurochem.*, 2012, **120**, 149–166.
17 L. E. Scott and C. Orvig, *Chem. Rev.*, 2009, **109**, 4885–4910.
18 E. L. Que, D. W. Domaille and C. J. Chang, *Chem. Rev.*, 2008, **108**, 1517–1549.
19 P. Faller, *ChemBioChem*, 2009, **10**, 2837–2845.
20 J. A. Duce and A. I. Bush, *Prog. Neurobiol.*, 2010, **92**, 1–18.
21 A. S. DeToma, S. Salamekh, A. Ramamoorthy and M. H. Lim, *Chem. Soc. Rev.*, 2012, **41**, 608–621.
22 P. Zatta, D. Drago, S. Bolognin and S. L. Sensi, *Trends Pharmacol. Sci.*, 2009, **30**, 346–355.
23 P. Faller and C. Hureau, *Dalton Trans.*, 2009, 1080–1094.
24 M. A. Telpoukhovskaia and C. Orvig, *Chem. Soc. Rev.*, 2013, **42**, 1836–1846.
25 R. A. Cherny, C. S. Atwood, M. E. Xilinas, D. N. Gray, W. D. Jones, C. A. McLean, K. J. Barnham, I. Volitakis, F. W. Fraser, Y.-S. Kim, X. Huang, L. E. Goldstein, R. D. Moir, J. T. Lim, K. Beyreuther, H. Zheng, R. E. Tanzi, C. L. Masters and A. I. Bush, *Neuron*, 2001, **30**, 665–676.
26 P. J. Crouch, D. J. Tew, T. Du, D. N. Nguyen, A. Caragounis, G. Filiz, R. E. Blake, I. A. Trounce, C. P. W. Soon, K. Laughton, K. A. Perez, Q.-X. Li, R. A. Cherny, C. L. Masters, K. J. Barnham and A. R. White, *J. Neurochem.*, 2009, **108**, 1198–1207.
27 C. W. Ritchie, A. I. Bush, A. Mackinnon, *et al.*, *Arch. Neurol.*, 2003, **60**, 1685–1691.
28 L. Lannfelt, K. Blennow, H. Zetterberg, S. Batsman, D. Ames, J. Harrison, C. L. Masters, S. Targum, A. I. Bush, R. Murdoch, J. Wilson and C. W. Ritchie, *Lancet Neurol.*, 2008, **7**, 779–786.
29 N. G. Faux, C. W. Ritchie, A. Gunn, A. Rembach, A. Tsatsanis, J. Bedo, J. Harrison, L. Lannfelt, K. Blennow, H. Zetterberg, M. Ingelsson, C. L. Masters, R. E. Tanzi, J. L. Cummings, C. M. Herd and A. I. Bush, *J. Alzheimer's Dis.*, 2010, **20**, 509–516.
30 A. S. Pithadia, A. Kochi, M. T. Soper, M. W. Beck, Y. Liu, S. Lee, A. S. DeToma, B. T. Ruotolo and M. H. Lim, *Inorg. Chem.*, 2012, **51**, 12959–12967.
31 C. Rodríguez-Rodríguez, M. Telpoukhovskaia and C. Orvig, *Coord. Chem. Rev.*, 2012, **256**, 2308–2332.
32 J. J. Braymer, J.-S. Choi, A. S. DeToma, C. Wang, K. Nam, J. W. Kampf, A. Ramamoorthy and M. H. Lim, *Inorg. Chem.*, 2011, **50**, 10724–10734.
33 Y. Liu, A. Kochi, A. S. Pithadia, S. Lee, Y. Nam, M. W. Beck, X. He, D. Lee and M. H. Lim, *Inorg. Chem.*, 2013, **52**, 8121–8130.
34 S. Lee, X. Zheng, J. Krishnamoorthy, M. G. Savelieff, H. M. Park, J. R. Brender, J. H. Kim, J. S. Derrick, A. Kochi, H. J. Lee, C. Kim, A. Ramamoorthy, M. T. Bowers and M. H. Lim, *J. Am. Chem. Soc.*, 2014, **136**, 299–310.
35 M. B. Goshe, Y. H. Chen and V. E. Anderson, *Biochemistry*, 2000, **39**, 1761–1770.
36 A. P. Breen and J. A. Murphy, *Free Radical Biol. Med.*, 1995, **18**, 1033–1077.
37 L.-W. Wang and M. R. Chance, *Anal. Chem.*, 2011, **83**, 7234–7241.
38 G. Xu and M. R. Chance, *Chem. Rev.*, 2007, **107**, 3514–3543.
39 C. L. Hawkins and M. J. Davies, *Biochim. Biophys. Acta, Bioenerg.*, 2001, **1504**, 196–219.
40 W. S. Bowen, W. E. Hill and J. S. Lodmell, *Methods*, 2001, **25**, 344–350.
41 H. Eguchi, Y. Ikeda, S. Koyota, K. Honke, K. Suzuki, J. M. C. Gutteridge and N. Taniguchi, *J. Biochem.*, 2002, **131**, 477–484.
42 S. Basak and V. Nagaraja, *Nucleic Acids Res.*, 2001, **29**, E105.
43 T. Kowalik-Jankowska, M. Ruta, K. Wisniewska, L. Lankiewicz and M. Dyba, *J. Inorg. Biochem.*, 2004, **98**, 940–950.
44 E. Heyduk and T. Heyduk, *Biochemistry*, 1994, **33**, 9643–9650.
45 E. R. Stadtman, *Annu. Rev. Biochem.*, 1993, **62**, 797–821.
46 S. D. Maleknia and K. M. Downard, *Chem. Soc. Rev.*, 2014, **43**, 3244–3258.
47 C. L. Hawkins and M. J. Davies, *J. Chem. Soc., Perkin Trans. 2*, 1998, 2617–2622.
48 D. T. Sawyer, *Coord. Chem. Rev.*, 1997, **165**, 297–313.
49 M. Strlic, J. Kolar, V.-S. Selih, D. Kocar and B. Pihlar, *Acta Chim. Slov.*, 2003, **50**, 619–632.
50 G. P. Anipsitakis and D. D. Dionysiou, *Environ. Sci. Technol.*, 2004, **38**, 3705–3712.
51 J. A. Simpson, K. H. Cheeseman, S. E. Smith and R. T. Dean, *Biochem. J.*, 1988, **254**, 519–523.
52 N. K. Urbanski and A. Beresewicz, *Acta Biochim. Pol.*, 2000, **47**, 951–962.

53 B. D. Schmidt and C. F. Meares, *Biochemistry*, 2002, **41**, 4186–4192.
54 K. B. Hall and R. O. Fox, *Methods*, 1999, **18**, 78–84.
55 M. A. Trakselis, S. C. Alley and F. T. Ishmael, *Bioconjugate Chem.*, 2005, **16**, 741–750.
56 G. M. Heilek and H. F. Noller, *Science*, 1996, **272**, 1659–1662.
57 L. Lancaster, M. C. Kiel, A. Kaji and H. F. Noller, *Cell*, 2002, **111**, 129–140.
58 P. A. MacFaul, D. D. M. Wayner and K. U. Ingold, *Acc. Chem. Res.*, 1998, **31**, 159–162.
59 W. M. Garrison, *Chem. Rev.*, 1987, **87**, 381–398.
60 R. T. Dean, S. P. Wolff and M. A. McElligott, *Free Radical Res. Commun.*, 1989, **7**, 97–103.
61 M. J. Davies, *Arch. Biochem. Biophys.*, 1996, **336**, 163–172.
62 E. R. Stadtman, *Methods Enzymol.*, 1995, **258**, 379–393.
63 C. J. Easton, *Chem. Rev.*, 1997, **97**, 53–82.
64 D. S. Rawat and J. M. Zaleski, *J. Am. Chem. Soc.*, 2001, **123**, 9675–9676.
65 T. Chandra, R. A. Allred, B. J. Kraft, L. M. Berreau and J. M. Zaleski, *Inorg. Chem.*, 2004, **43**, 411–420.
66 S. E. Lindahl, H. Park, M. Pink and J. M. Zaleski, *J. Am. Chem. Soc.*, 2013, **135**, 3826–3833.
67 P. J. Benites, R. C. Holmberg, D. S. Rawat, B. J. Kraft, L. J. Klein, D. G. Peters, H. H. Thorp and J. M. Zaleski, *J. Am. Chem. Soc.*, 2003, **125**, 6434–6446.
68 B. J. Kraft, N. L. Coalter, M. Nath, A. E. Clark, A. R. Siedle, J. C. Huffman and J. M. Zaleski, *Inorg. Chem.*, 2003, **42**, 1663–1672.
69 J. M. Walker, L. Gou, S. Bhattacharyya, S. E. Lindahl and J. M. Zaleski, *Chem. Mater.*, 2011, **23**, 5275–5281.
70 S. M. Routt, J. Zhu, J. M. Zaleski and J. R. Dynlacht, *Int. J. Hyperthermia*, 2011, **27**, 435–444.
71 W. C. Dewey, S. A. Sapareto and D. A. Betten, *Radiat. Res.*, 1978, **76**, 48–59.
72 P. M. Corry, S. Robinson and S. Getz, *Radiology*, 1977, **123**, 475–482.
73 E. Dikomey and J. Franzke, *Int. J. Radiat. Biol.*, 1992, **61**, 221–233.
74 R. S. L. Wong, J. R. Dynlacht, B. Cedervall and W. C. Dewey, *Int. J. Radiat. Biol.*, 1995, **68**, 141–152.
75 W. L. Titsworth, G. J. A. Murad, B. L. Hoh and M. Rahman, *Anticancer Res.*, 2014, **34**, 565–574.
76 D. M. Welsh, *Crit. Care Nurs. Clin.*, 1995, **7**, 115–123.
77 M. H. Falk and R. D. Issels, *Int. J. Hyperthermia*, 2001, **17**, 1–18.
78 Y. Anzai, R. Lufkin, A. DeSalles, D. R. Hamilton, K. Farahani and K. L. Black, *Am. J. Neuroradiol.*, 1995, **16**, 39–48.
79 C. Rodriguez-Rodriguez, N. Sanchez de Groot, A. Rimola, A. Alvarez-Larena, V. Lloveras, J. Vidal-Gancedo, S. Ventura, J. Vendrell, M. Sodupe and P. Gonzalez-Duarte, *J. Am. Chem. Soc.*, 2009, **131**, 1436–1451.
80 A. K. Sharma, S. T. Pavlova, J. Kim, D. Finkelstein, N. J. Hawco, N. P. Rath, J. Kim and L. M. Mirica, *J. Am. Chem. Soc.*, 2012, **134**, 6625–6636.
81 L. Di, E. H. Kerns, K. Fan, O. J. McConnell and G. T. Carter, *Eur. J. Med. Chem.*, 2003, **38**, 223–232.
82 A. Avdeef, S. Bendels, L. Di, B. Faller, M. Kansy, K. Sugano and Y. Yamauchi, *J. Pharm. Sci.*, 2007, **96**, 2893–2909.
83 D. E. Clark and S. D. Pickett, *Drug Discovery Today*, 2000, **5**, 49–58.
84 C. A. Lipinski, F. Lombardo, B. W. Dominy and P. J. Feeney, *Adv. Drug Delivery Rev.*, 2001, **46**, 3–26.
85 *BBB Protocol and Test Compounds*, pIon, Inc., Woburn, MA, 2009.
86 J. Masuoka, J. Hegenauer, B. R. Van Dyke and P. Saltman, *J. Biol. Chem.*, 1993, **268**, 21533–21537.
87 L. D. Pettit and J. L. M. Swash, *J. Chem. Soc., Dalton Trans.*, 1976, 588–594.
88 H. Zhang, C.-S. Liu, X.-H. Bu and M. Yang, *J. Inorg. Biochem.*, 2005, **99**, 1119–1125.
89 E. Gaggelli, H. Kozlowski, D. Valensin and G. Valensin, *Chem. Rev.*, 2006, **106**, 1995–2044.
90 M. T. Soper, A. S. DeToma, S.-J. Hyung, M. H. Lim and B. T. Ruotolo, *Phys. Chem. Chem. Phys.*, 2013, **15**, 8952–8961.
91 J. Coon, J. Shabanowitz, D. Hunt and J. P. Syka, *J. Am. Soc. Mass Spectrom.*, 2005, **16**, 880–882.
92 E. Bagheri-Majdi, Y. Ke, G. Orlova, I. K. Chu, A. C. Hopkinson and K. W. M. Siu, *J. Phys. Chem. B*, 2004, **108**, 11170–11181.
93 R. E. Bossio, R. R. Hudgins and A. G. Marshall, *J. Phys. Chem. B*, 2003, **107**, 3284–3289.
94 T.-Y. Huang, J. F. Emory, R. A. J. O'Hair and S. A. McLuckey, *Anal. Chem.*, 2006, **78**, 7387–7391.